Effect of Anti-Microbial Oligomers on HEK293A Cell Membrane

Roya Lahiji[*], Yan Li[**], Gregory Tew[**] and Mark Banaszak Holl[***]
[*]Department of Physics, University of Michigan, Ann Arbor, MI 48109; lahijir@umich.edu
[**]Department of Polymer Science and Engineering, University of Massachusetts Amherst, MA 01003
[***]Department of Chemistry, University of Michigan, Ann Arbor, MI 48109

ABSTRACT

This paper presents results from a study of the interaction of amphiphilic phenylene ethynylene antimicrobial oligomer (AMO-1, 2 and 3), a synthetic antimicrobial peptides (AMP) analogs, with HEK 293A (human embryonic kidney) cell line using a high throughput whole cell patch clamp technique. Cells are patched in an IonFlux 16 instrument and electric response of the cells, due to the damage or pore formation, in the cell membrane is monitored. On average, the increase in the electric signal was 25±5 nA for AMO-1, for AMO-2 was 10±2 nA and for AMO-3 was multiples of few nanoAmpere current steps that added up to 25±5 nA. Our results show that the degree of interaction and disruption of the AMOs with HEK 293A cells are different and dependent on the hydrophobic chain length of them.

Keywords: Antimicrobial Oligomers, Cell Membrane, Automated Patch Clamp, Ionflux 16, HEK 293A Cells.

1 INTRODUCTION

Amphiphilic phenylene ethynylene antimicrobial oligomers (AMO-1, 2 and 3) are synthetic antimicrobial peptides (AMP) analogs, which are unique as they are amphipathic and cationic.[1-4] Due to their amino acid composition, amphipathicity, charge and size they can easily attach to and insert into membrane bilayers to form pores.[2] Designing synthetic antimicrobial systems that could help to mitigate, combat and/or eliminate infectious diseases leading to an improvement in the state of our well-being remains a challenging area.[5] It is critical to understand how AMO molecules interact with individual cells and evaluate their state of toxicity. It is well established that cationic molecules disrupt the cell membrane [6-10] and understood that AMO-3 creates well defined holes that are 3.4 nm in diameter.[11, 12] Studies on lipid bilayers interacting with AMO 1, 2 and 3 suggest that there are clear differences between each kind of AMO.[11, 12] Results indicate that the lipid composition and even lipid ordering within the cell membrane impacts the level of interaction of these molecules and may have important consequences on biological selectivity.[11] Yang et al report on AMO-1 being inactive, while AMO-2 is active and AMO-3 is selectively active against red blood cells. To date, these studies have been performed on model membranes and therefore extrapolating the observations into real world phenomena need be done with extra caution.

The whole cell patch clamp technique [13] is one of the precise methods to monitor the changes in the ion flow of individual live cells. The electrical conductance signal is a very precise way to understand the cell membrane poration and damage. Depending on the type of cell interaction with the particles, the cell membrane might either disrupt and recover or unable to recover leading to cell death. Either of the cases cause changes in the electric signal collected from the cells, and collectively the data shows the behavior of cells in response of the particulates. Although whole cell patch clamp is a highly sensitive technique, it is very time consuming and slow. On the other hand, high throughput cell patch clamp [14-16] uses very similar techniques to whole cell patch clamp, with the difference being in the number of the cells studied simultaneously. IonFlux 16 (IF16) [15] is an instrument which can patch up to 320 cells at once and monitor their electric responses. With the IF16, besides being able to study multiple cells at the same time, one can easily vary and compare the experimental conditions and therefore have a more statistically accurate study on the cell behavior during interaction with particles.

The cell membrane interaction with AMO molecules was monitored through changes in the electric conduction using the IF16 technique. Here we report on the comparison of the interaction of each AMO molecule with HEK 293A cell membrane. Besides introducing high throughput patch clamp technique to study cell membrane behaviors, this study helps to understand how different hydrophobic chain length of AMOs can change cell membrane interactions.

2 MATERIALS AND METHODS

Human embryonic kidney cells, HEK 293A (from Invitrogen, Carlsbad, CA), were chosen for this study. These cells are easy to grow, and their doubling time is 24 hours. Dulbecco's modified Eagle's medium (DMEM) (Gibco, Eggenstein, Germany) supplemented with 10% fetal bovine serum (FBS), 1% MEM nonessential amino acids (NEAA), and 1% penicillin-streptomycin were used to grow the cells in a monolayer in an incubator set to 37^{o}C with 5% CO_2. The media was changed every 3-4 days. (All the supplements have been purchased from Fisher Scientific.)

Cells were cultured in a T175 sterile tissue culture flask (BD Falcon) and used for experiments when a monolayer was grown and the flask was ~90% confluent. To detach the cells trypsin (Gibco) with 4-5 min incubation time was used. After trypsinization with DMEM and centrifugation, the cells were introduced to room temperature 293 SFMII media (Invitrogen). The 293 SFMII media is a serum free media which helps in dissociation of cells to create a single cell suspension. This is a critical step, as cells need to be individual in order to increase the trapping efficiency in the microfluidic plates used in the study. A second centrifugation was followed after titration of the cells in the SFMII media. At the final stage, cells were titrated in the external cellular solution (ECS) (with the following recipe: KCl 4mM, NaCl 138 mM, $MgCl_2$ 1 mM, $CaCl_2$ 1.8 mM, glucose (Dextrose) 5.6 mM, HEPES 10 mM that is adjusted to PH 7.45 with addition of NaOH) at the right concentration such that there were a total of 8-10 million individual cells per ml of ECS.

The AMO molecules were synthesized according to previously reported procedures. Typical purity of the AMOs, as found by HPLC, is 98%, and the characterizations of AMO molecules are in accordance with the literature. (Patent US2005287108(A1), J. Phys. Chem. B 2008, 112, 3495-3502). The AMO chemical structure is as shown in Figure 1(a).

3 RESULTS AND DISCUSSION

An automated patch clamp, IF16 (Fluxion Biosciences, CA), was used for this study. This technique is similar to the whole cell patch clamp technique with a few added benefits. The advantage of using such a system instead of whole cell patch clamp is the ease in acquiring data from multiple cells at once, as well as the ability to flow a total of 8 different compounds at the same time or separately as experiment calls, and easily varying experimental conditions. Figure 1(b) shows a diagram of one, out of 8, patterns in the plate used for the experiments.

To prepare a plate, all the wells were filled with 250 µl of the appropriate compounds. Internal cellular solution (ICS) (with the following recipe: K*Asp 100 mM, KCl 30 mM, $MgCl_2$ $6H_2O$ 5mM, EGTA 5 mM, Trip-ATP 4mM, HEPES 10 mM that is adjusted to PH of 7.2 with addition of KOH) was added to the T1 and T2 zones, while out-well stayed empty and In-well received 250 µl of the cell suspension in ECS. In our experiments only two compound wells were used. Usually C1 was filled with ECS and C2 was filled with either of the AMOs. The rest of the compound wells were not used and filled with PBS.

By adjusting the applied pressure settings (a pulsed pressure between 0 and 0.25 psi for 0.8 seconds for a total of 85 seconds in the main channel and trap pressure of 6 psi for the trap channel for a total of 85 seconds) in the IonFlux software, twenty cells were trapped automatically in each trapping zone of a plate. There were a total of 16 trapping zones in a plate. This is where having well separated individual cells plays a critical role in trapping efficiency and produces a better outcome of the experiment. After trapping the cells were exposed to the compounds. Since AMO molecules were dissolved in a mixture of 0.5% (v/v) of Dimethyl sulfoxide (DMSO) and ECS solution we ran this compound in 2 patterns of each plate as a control. We designed the experiments principally with two specific setups. In one scenario, the cells were exposed to AMO molecules in short pulses then washed with ECS (data not shown).

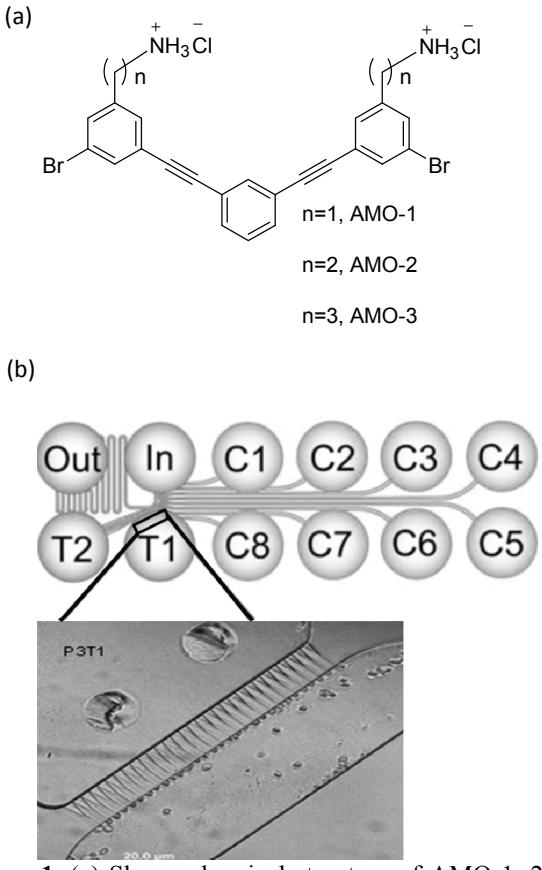

Figure 1. (a) Shows chemical structure of AMO-1, 2, and 3. In (b) diagram of one out of eight patterns in an Ionflux 16 plate used for the experiments is shown. There are 8 wells assigned for compounds, marked with C1-C8. Two wells labeled with T1 and T2 are the two trapping zones. There is one In-well, where the cells are introduced, and one out-well, which is used as a waste channel. The microscope view of T1 shows cells trapped by the microchannels.

Here cell recovery from exposure to the AMO molecules was monitored. Basically, the return of the conductance signal to the original value, when cells were washed with ECS, after exposure to AMO indicates recovery of the cells. The pulses range from 30 seconds to 240 seconds. In another experimental scenario, the exposure time was extended; cells were exposed to AMO molecules for up to a total of 12 minutes. This protocol gives information on how the membrane of live cells reacted with AMO molecules over time. In order to avoid cells losing their seal to the

microchannel we did not extend the exposure time farther than 18 minutes in total. It is also important to keep in mind that the data collected from each of the trapping zones is an average of the 20 cells in that specific trapping zone, not from an individual cell. In this type of study we are presented with an average overview of the whole phenomenon.

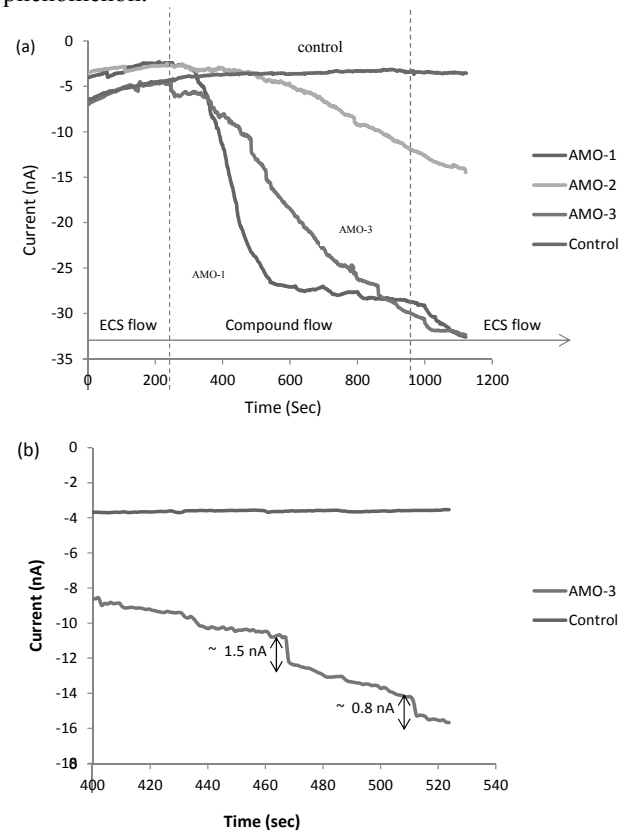

Figure 2. (a) Shows membrane current trace of the HEK 293A cells when exposed to AMO compounds. At time t=0 ECS started to flow to stabilize the cells. At t=240 sec the compound (either of AMOs or the DMSO control) started to flow. At t=960 sec the flow of compound stopped and ECS was flown to monitor cell viability and ability to recover its membrane. 0.5% (v/v) of DMSO and ECS were ran as the controls and was steady throughout the time, showing that any other fluctuations were real changes in the cell membrane. AMO-2 appeared to be less toxic compared to AMO-1 and AMO-3. AMO-3 was as toxic as AMO-1, however the disruption effect were more stepwise than AMO-1. (b) Shows representative current steps when AMO-3 interacted with the membrane of HEK 293A cells.

The results of this study suggest that the interaction of AMO with HEK 293A cell membrane can be described as one that disrupts the cell membrane, however with a large degree of order. The study showed that the level of interaction depended on the hydrophobic chain length. In the case of exposing the live cells to the AMO molecules for short exposure times, it was observed that AMO-1 was the most toxic (see figure 2(a)). In the first minutes of exposure the membrane disruption was almost irreversible, and cells were unable to reseal themselves to maintain their initial conductance. The very similar phenomenon happened for the AMO-3 molecule, however not as rapid as in the case of AMO-1 molecules. For AMO-3 molecules the toxic effects started after about 4-5 minutes of exposure, yet the cell membrane was able to reseal and recover. When the exposure was continued, it was determined that the cell membrane lost the ability to recover, possibly due to the increase in the number of disruptive events. Conversely, the effect of AMO-2 was less toxic, however cells did not retain their ability to reseal and recover after exposure. Figure 2(a) shows the effect of each of the AMOs on the membrane of HEK 293A cells.

As previously mentioned, the conductance signal was used to identify the events that take place at the cell membrane level. In order to better compare the effects of the AMO molecules, the current increase for each case was calculated. When cells were exposed to AMO-1 molecules the total current increase was on average 25±5 nA, while in the case of the AMO-3 molecules the current increase was multiples of small incremental steps (see figure 2(b)), each a few nanoAmperes in magnitude, which added up to the same current increase as for AMO-1. The current increase in the case of AMO-2 molecules was in the range of 10±2 nA.

These membrane effects can be explained as either a physical hole in the membrane or as an incorporation of the compound in the cell membrane that disrupted the structure and allowed ion flow. If the first case is considered, then using the measured increases in current we can estimate the hole size formation. Figure 2(b) shows a zoomed in image of the current steps for the case of AMO-3. Table (1) summarizes the correlation between the current steps with the hole size formation. To estimate the hole size the following equation [6, 17] has been used.

$$r = \frac{g_{step}}{4}\left(1 \pm \sqrt{\rho^2 + 16\frac{\rho l}{\pi g_{step}}}\right)$$

Here r is the radius of the hole, g_{step} is the conductance of the current step, l is the hole length or thickness of the membrane (approximated to be 7 nm), ρ is the resistivity of the solution, which is approximately 50 Ωcm. g_{step} can also be calculated from $g_{step} = \frac{\Delta I_{step}}{(E_m - E_{rev})}$, where ΔI_{step} is the magnitude of the current step, E_m is the holding potential (set at -70 mV), and E_{rev} is the reversal potential that is considered to be zero mV from the I-V relationships.

The current increase in the case of AMO-3, as shown in Fig 2, was due to the addition of multiple small current steps in the range of 0.5 nA to 2 nA. As shown in Table 1, each step corresponds to a hole with the diameter of 4.3-20 nm. Depending on the number of these disruptive events in the membrane, this might be the reason for cell damage and loss of the reseal ability.

Table 1. Relation between the sizes of the holes (diameter) formed in the cell membrane due to the interaction with AMOs based on the current step sizes similar to the one shown in Figure 2(b). Equation 1 was used to calculate these ranges.

Current (nA)	0-0.5	0.5-1	1-1.5	1.5-2	2-2.5	2.5-3	3-3.5	3.5-4	4-4.5
Hole size (nm)	4.3-7.7	8.6-12.3	13.1-16.5	17.3-20.5	21.3-24.4	25.1-28.2	28.9-32	32.7-35.7	36.4-39.4

4 CONCLUSION

In this study we compared the effect of exposure of three kinds of AMOs, each having a different hydrophobic chain length, on the membrane of the HEK 293A cell line. The method used for this study tracks the electrical conduction signal from ion flow across the cell membrane and therefore provides a very precise technique to characterize cell membrane responses. The overall behavior can be described as cells losing their ability to reseal and recover from increased porosity introduced by the AMOs. Although the end result is similar, each case has its own progression steps. The process of damage in the case of AMO-1 is immediate and sharp, meaning, as soon as AMO-1 was introduced, cells lost their integrity and transmembrane current increased rapidly. In the case of AMO-2, the cells started to porate a few minutes after being introduced to the AMO-2. Although AMO-2 seemed to be less toxic than the other AMOs, the process was irreversible and the current increased as the exposure time progressed. AMO-3, likewise, affected the membrane; however the current increase was stepwise with the chance of recovery in the first couple of minutes of exposure. Overall, the level of cell membrane disruption with AMO-3 was the same as the case of AMO-1.

Utilizing the IF16 instrument provided the advantage to monitor the AMO molecules effect in vitro in live cells. We were able to systematically vary the experimental conditions, such as flow of compound (AMO molecules) followed by flow of ECS for a chance of recovery of membrane. Reported observations indicate the importance of the design of the molecules and nanoparticles and how chain length can affect the type of interaction it will have with the cell membrane. This study also helps in understanding the antimicrobial-membrane interactions, which is a critical step towards the design of more predictive synthetic AMP analogs for the challenges ahead to effectively mitigate, combat and/or eliminate infectious diseases.

ACKNOWLEDGMENTS

The authors would like to thank Fluxion Biosciences, specifically Dr. Juliette Johnson, Dr. Cristian Ionescu-Zanetti and Dr. Steve Smith for their support and useful discussions regarding cell preparation and optimal function of the IF16 instrument.

REFERENCES

1. Boman, H.G., Innate immunity and the normal microflora. Immunological Reviews, 2000. 173: p. 5-16.
2. Brogden, K.A., Antimicrobial peptides: Pore formers or metabolic inhibitors in bacteria? Nature Reviews Microbiology, 2005. 3(3): p. 238-250.
3. Hancock, R.E.W. and R. Lehrer, Cationic peptides: a new source of antibiotics. Trends in Biotechnology, 1998. 16(2): p. 82-88.
4. Hancock, R.E.W. and A. Rozek, Role of membranes in the activities of antimicrobial cationic peptides. FEMS Microbiology Letters, 2002. 206: p. 143-149.
5. Mu˜noz-Bonilla, A. and M. Fernández-García, Polymeric materials with antimicrobial activity. Progress in Polymer Science, 2012. 37(2): p. 281–339.
6. Chen, J., et al., Cationic Nanoparticles Induce Nanoscale Disruption in Living Cell Plasma Membranes. The Journal of Physical Chemistry B, 2009. 113(32): p. 11179-11185.
7. Hong, S., et al., Interaction of poly(amidoamine) dendrimers with supported lipid bilayers and cells: hole formation and the relation to transport. Bioconjug Chem, 2004. 15(4): p. 774-782.
8. Leroueil, P.R., et al., Wide Varieties of Cationic Nanoparticles Induce Defects in Supported Lipid Bilayers. Nano Letters, 2008. 8(2): p. 420-424.
9. Leroueil, P.R., et al., Nanoparticle Interaction with Biological Membranes: Does Nanotechnology Present a Janus Face? Accounts of Chemical Research, 2007. 40(5): p. 335-342.
10. Mecke, A., et al., Direct observation of lipid bilayer disruption by poly(amidoamine) dendrimers. Chemistry and Physics of Lipids, 2004. 132(1): p. 3-14.
11. Arnt, L., et al., Membrane Activity of Biomimetic Facially Amphiphilic Antibiotics. J. Phys. Chem. B, 2006. 110(8): p. 3527-3532.
12. Yang, L.H., et al., Synthetic antimicrobial, oligomers induce a composition-dependent topological transition in membranes. Journal of the American Chemical Society, 2007. 129(40): p. 12141-12147.
13. Fertig, N., R.H. Blick, and J.C. Behrends, Whole cell patch clamp recording performed on a planar glass chip. Biophysical Journal, 2002. 82(6): p. 3056-3062.
14. Farre, C. and N. Fertig, HTS techniques for patch clamp-based ion channel screening - advances and economy. Expert Opinion on Drug Discovery, 2012. 7(6): p. 515-524.
15. Golden, A.P., et al., IonFlux: A Microfluidic Patch Clamp System Evaluated with Human Ether-à-go-go Related Gene Channel Physiology and Pharmacology. ASSAY and Drug Development Technologies, 2011. 9(6): p. 608-619.
16. Kodandaramaiah, S.B., et al., Automated whole-cell patch-clamp electrophysiology of neurons in vivo. Nature Methods, 2012. 9(6): p. 585.
17. Noronha, F.S.M., et al., Infect. Immun, 2000. 68: p. 4578.